Phase Separation in Ternary Systems Solvent-Polymer 1-Polymer 2. 4. Critical Points of Scott Systems

K. Šolc,* Y.-H. Huang, and Y. C. Yang†

Michigan Molecular Institute, Midland, Michigan 48640. *Received January 18, 1989; Revised Manuscript Received April 5, 1989*

ABSTRACT: In ternary systems, explicit critical point (CP) formulas have been known for only one subclass, representative of solutions of two partly incompatible polymers. Rigorous recasting of approximate critical equations obtained for this case by Scott has shown that, to qualify, the system's three interaction parameters have to match certain relation **S**. A detailed analysis of such systems is carried out. *On the isothermal level*, criteria are derived for the *coexistence* of Scott critical points (SCP) with homogeneous and heterogeneous double critical points (HODCPs and HEDCPs) at the same temperature. Since HODCPs mark important events of phase behavior, such as coalescence of two growing unstable regions, their criteria are useful for predicting the spinodal and binodal patterns. Conditions for a SCP overlapping with an HEDCP, on the other hand, outline the onset of thermodynamic instability in SCPs. Both criteria are given in terms of $\bar{g}$, the mean polymer–solvent interaction parameter, a quantity so far considered as not too important. Critical behavior of a given system *over a range of temperatures* depends on the degree of system's adherence to the required relation **S**. In hypothetical *strictly Scott systems* satisfying **S** at all temperatures, the Scott critical line (SCL, locus of SCPs) is trivial, and the HEDCP on it (if any) marks a singular point where SCL abruptly transforms into a "regular" transverse critical line (TCL), usually exiting through the two binary polymer–solvent CPs. For *real Scott systems*, a first-order perturbation theory is developed to account for the less than perfect match of the condition **S**. The perturbation theory fits very well the exact computation of the "SCL", now deflected from its ideal position, and the simple results should be valuable for data interpretation. The relaxation of condition **S** also reveals the singular nature of the above Scott HEDCP: with critical lines retreating from it, and the transition between the "SCL" and TCL becoming smooth, the discontinuity around HEDCP becomes clearly visible. Numerous computed spinodal and critical-line diagrams are given to document the predicted behavior.

1. Introduction

Until recently, explicit critical state relations had been reported for only one subclass of ternary systems solvent–polymer 1–polymer 2, typical of solutions of two segregating polymers.[1] In triangular composition diagram of such systems, the miscibility gap based on polymer 1–polymer 2 binary axis extends into the ternary space. Using Flory–Huggins thermodynamics,[2] Scott discovered approximate relations characterizing in some instances the critical point (CP) of such systems[1]

$$w_{2,S} \approx \rho_1/(\rho_1 + \rho_2) \tag{1}$$

$$g_x \approx (\rho_1 + \rho_2)^2/2\varphi r_1 r_2 \tag{2}$$

where g_x is the polymer 1–polymer 2 interaction parameter (per segment), φ is the total volume fraction of the polymeric solute in the solution, w_2 is the volume fraction of polymer 2 in the mixture of polymers, r_i is the relative chain length of polymer i, and $\rho_i = r_i^{1/2}$. According to eq 1 and 2, (i) such CPs are defined only along the constant-composition line $w_{2,S}$ (see Figure 1), and (ii) the critical polymer volume fraction φ is inversely proportional to g_x. Thus, Scott concluded that "the main contribution of the solvent is purely that of lowering the critical solution temperature by dilution; the exact nature of the solvent is of only secondary importance".[1]

For a long time the only critical formulas available for ternary systems, relations 1 and 2 have been popular particularly among experimentalists interested in solutions of incompatible polymer mixtures.[3] Yet it has never been clear to what extent these equations were truly applicable to a given case; it was obvious that not all treated systems could satisfy the assumptions under which eq 1 and 2 were valid.

Only recently it was shown by rigorous analysis of critical state[4] that eq 1 and 2 are actually *exact* if also

$$\Delta g = g_x(\rho_1 - \rho_2)/(\rho_1 + \rho_2) \tag{3}$$

where Δg is the difference between the two polymer–solvent interaction parameters, $\Delta g \equiv g_2 - g_1$. The additional condition (3), in the Abstract denoted by **S**, replaces the uncalled-for restrictions imposed on the magnitude of some variables in the original Scott paper.[1] Of course, another requirement guaranteeing the appearance of the CP *within* the triangle of composition is that the repulsive interactions polymer 1–polymer 2 be intense enough to cause the phase separation at least in the bulk polymer (cf. eq 2)

$$g_x \geq g_{x,\min} = (\rho_1 + \rho_2)^2/2r_1 r_2 \tag{4}$$

On the other hand, the mean value of the polymer–solvent interaction parameter, $\bar{g} \equiv (g_1 + g_2)/2$, at a Scott CP can be arbitrary. It is only in this sense that "the exact nature of the solvent" is unimportant, as stated by Scott;[1] however, the character of the solvent *is* important for satisfying eq 3.

Since it is highly improbable that any "real" Flory–Huggins system would fit eq 3 exactly at all times, it is desirable for any given case (a) to clearly define the degree of adherence to eq 3 and (b) to develop a perturbation theory based on deviations from eq 3. Consequently, we propose the following nomenclature:

(i) Only the CPs satisfying eq 1–3 *exactly* shall be called *Scott* CPs, as opposed to *regular* CPs that do not match this condition. CPs fitting eq 1–3 only *approximately* could be called *perturbed Scott* CPs. It is interesting to note that eq 3 is a source of an asymmetry: For instance, if the chain length of polymer 2 is larger than that of polymer 1, then a Scott CP can be observed only if the employed solvent is better for polymer 2 than for polymer 1 ($g_2 < g_1$).

(ii) System classification should be based on behavior over a range of temperatures. For practical reasons and in the spirit of Scott's original work,[1] a so-called *Scott system* will be required to match eq 1–3 only loosely. On the other hand, a hypothetical reference system satisfying

†Present address: PPG Fiberglass Research Center, P.O. Box 2844, Pittsburgh, PA 15230.

0024-9297/89/2222-4334$01.50/0

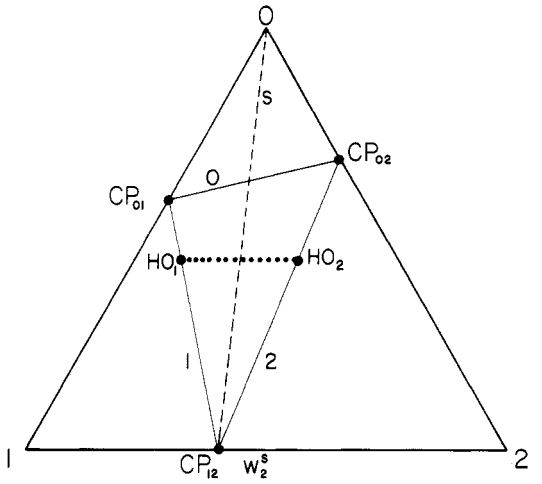

Figure 1. Composition triangle for the system $r_1 = 2, r_2 = 5$: CP_{ij}, binary CP for a mixture of components i and j; s, linear locus of Scott CPs, eq 1; (—) linear loci of homogeneous double CPs (HODCPs) of the types 0, 1, and 2; $\overline{0\text{–}CP_{01}\text{–}CP_{12}\text{–}CP_{02}\text{–}0}$ trapezium boundary of the projected critical ξ^2-surface 0; HO_1, HO_2, two HODCPs bounding the line of the w_2 scan (···) of surface 0 for $\varphi = 0.55$ (cf. Figure 3).

eq 3 at all temperatures will be called a *strictly Scott system* (SSS).

Development of a perturbation theory for Scott systems is one of the main objectives of this report. The results should provide a more realistic basis for interpretation of data on segregating systems, compared to the present practice. Another goal is a detailed analysis of SSSs, particularly how this peculiar subgroup fits into the infinite spectrum of all other ternary systems, what are the criteria for coexistence of Scott CPs with some other special CPs, what is their stability, what is the interaction between the Scott critical line and "regular" critical line, etc.

2. Critical Point Diagrams in Interaction Space

In a Flory–Huggins ternary system solvent (0)–polymer 1 (1)–polymer 2 (2) the critical state is defined by the following three functions[4]

$$F_c \equiv \Phi^2\langle r\xi\rangle^3 - \langle r^2\xi^3\rangle = 0 \tag{5}$$

$$G_c \equiv \xi^2(1 - \varphi_2 r_2 P) - (1 - \varphi_1 r_1 M) = 0 \tag{6}$$

$$H_c \equiv \xi^2 + 1 + \varphi\{\xi\langle r\xi\rangle[(2/\varphi_0) - 4\bar{g}] + w_1 r_1 P + \xi^2 w_2 r_2 M\} = 0 \tag{7}$$

where φ_i is the volume fraction of the component i (ordered so that $r_2 \geq r_1$), and $\varphi = \varphi_1 + \varphi_2 = 1 - \varphi_0$; Φ stands for the ratio $\Phi \equiv \varphi/\varphi_0$; the symbol $\langle\rangle$ denotes a statistical moment of the mixed-polymer distribution

$$\langle r^i\xi^j\rangle = w_1 r_1{}^i\xi^{-j} + w_2 r_2{}^i\xi^j$$

ξ^2 is the critical ratio of Flory's separation factors[2]

$$\xi^2 \equiv \lim_{\sigma_m \to 0} \sigma_2/\sigma_1$$

and P and M denote the sum and the difference of the two "heteroparameters" g_x and Δg, respectively, $P \equiv g_x + \Delta g$, and $M \equiv g_x - \Delta g$. Note that if polymers 1 and 2 are of the same chemical nature, $g_x = \Delta g = P = M = 0$. All interaction parameters are in principle functions of temperature, but they are assumed to be independent of the system composition.

Critical point diagrams illustrate the relation between critical points (CPs) and variables on a global scale (i.e., not just for a particular ternary system, but rather for an ensemble of all imaginable ternary systems, in this paper restricted to having a given set of chain lengths r_1, r_2). The simplest and most compact of such diagrams is the critical ξ^2–surface, indispensable for good understanding of homogeneous double critical points (HODCPs), shapes of critical lines, etc. From eq 5, cubic in ξ^2, the ξ^2 value is fixed just by the critical composition φ and w_2, and the locus of all CPs thus takes form of a thrice-folded ξ^2-*surface* erected above the composition triangle.[4] From the practical point of view, however, this diagram is not too helpful; it would be preferable to employ other quantities such as interaction parameters, even when the locus of CPs in such coordinates expands its dimensionality to a 3D *space* [as the six critical variables φ, w_2, ξ^2, $\bar{g}$, Δg, and g_x are tied by three equations (5–7), leaving 3 degrees of freedom].

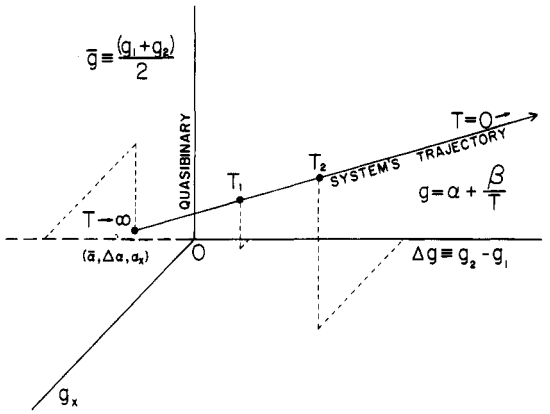

Figure 2. Interaction space (g-space) of ternary systems. For the common type of temperature dependence, $g = \alpha + \beta/T$, the trajectory of a particular system is linear. All quasi-binary systems coincide with the $\bar{g}$ axis.

One interesting option is to employ the 3D space of interaction parameters $\bar{g}$, Δg, and g_x (further referred to as the *interaction space*, or *g-space*), with $\bar{g}$ plotted as a vertical (Figure 2). Each particular system with known $g(T)$ dependence is here represented by its own spatial curve, or *trajectory*, with temperature as the parameter, that fully defines the phase behavior over a range of temperatures. On the other hand, the g-space contains some structural features, determined by critical eq 5–7 in combination with other relations, such as the HODCP surfaces,[5] the half-plane of Scott CPs, and the surface of heterogeneous double critical points (HEDCPs),[6] that mark important events in the phase development of a system. Consequently, one can better understand, and even anticipate, the phase behavior of a given system just by examining the course of its trajectory relative to the above-mentioned structural features of the g-space.

When considering the relation between loci of CPs in these two kinds of critical point diagrams, it is important to realize that there is no one-to-one correspondence between points of the critical ξ^2-surface with fixed φ, w_2, and ξ^2, and points of the critical g-space $\bar{g}$, Δg, g_x. For instance, a *point* of the ξ^2-surface projects into the g-space as a *straight line* (call it an isopleth) since eq 6 and 7 are linear in all interaction parameters. Physically speaking this means that a specific CP in the composition space can be realized by an infinite number of combinations of the three interaction parameters. On the other hand, some of these isopleths *may* intersect one another. Consequently, a point of the g-space may be shared by several isopleths and mapped into the composition space as *several* (but *not* an infinite number of) "unrelated" critical points. This is also obvious from the well-known fact that at a given temperature (i.e., a given point in g-space) a ternary system's phase diagram may contain several CPs on its binodals.

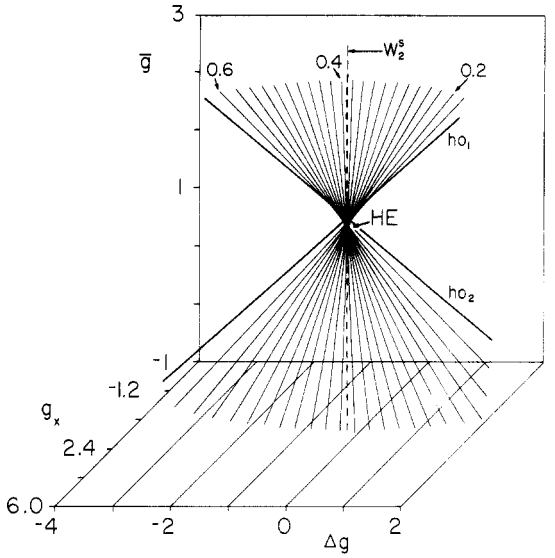

Figure 3. Sequence of critical isopleths in g-space for CPs with $\varphi = 0.55$ located on the ξ^2-surface 0, for a system $r_1 = 2$, $r_2 = 5$: (—) isopleths incremented by $\Delta w_2 = 0.02$ for the interval $0.18 \leq w_2 \leq 0.60$; (—) two bounding HODCP lines for the points HO_1 and HO_2 of Figure 1 with $w_2 \approx 0.1633$ and $w_2 \approx 0.6116$; (---) vertical line for Scott systems; HE, Scott HEDCP (eq 13).

In our analysis,[4] the Scott CPs are defined by both moments of eq 5 becoming zero; from this condition it is deduced that

$$\xi_S^2 = -\rho_1/\rho_2 \tag{8}$$

and $w_2 = w_{2,S}$ of eq 1. It is apparent that, in this case, the relation 5 is no longer useful for determination of Φ and φ. Other formulas can be abbreviated by introducing two parameters employed before:[5]

$$\mu = (\rho_2 - \rho_1)/2\rho_1\rho_2 \qquad \nu = (\rho_1 + \rho_2)/2\rho_1\rho_2 \tag{9a}$$

Equation 6 then yields the relation 2, transcribed as

$$g_x\varphi = 2\nu^2 \tag{9b}$$

while eq 7 reduces to eq 3, also written as

$$\Delta g = -g_x\mu/\nu \tag{9c}$$

No critical equation is left to fix $\bar{g}$. These relations indicate that the locus of all Scott CPs in the g-space is a *vertical half-plane* of orientation $g_x/\Delta g = -\nu/\mu$, extending from $g_{x,min} = 2\nu^2$ (cf. eq 4) up to $g_x \to +\infty$, with φ correspondingly decreasing from 1 to 0 (cf. eq 9b).

Since all Scott CPs lie on the line of constant polymer composition, $w_2 = w_{2,S}$, a convenient way to examine their neighborhood is to scan the composition space in transverse direction by stepping w_2 at constant φ. Each CP generates a line in the interaction space, and their collection forms a surface as shown in Figure 3 for $\varphi = 0.55$. For better clarity only its relevant part is shown—namely the CPs located on the ξ^2-surface 0 (dotted in Figure 1)—since the Scott CPs can reside nowhere else. The dashed line in Figure 3 corresponding to the Scott composition, $w_{2,S} \approx 0.3874$, is hand-plotted at $g_x \approx 1.211$ and $\Delta g \approx -0.2727$ (eq 9b and 9c) as a vertical (since $\bar{g}$ is arbitrary), and it fits smoothly into the family of computer-generated lines for $w_2 \neq w_{2,S}$. Its unique vertical orientation explains a long-standing puzzle concerning an apparent discontinuity in degrees of freedom of CPs: Why selecting a composition (φ,w_2) for a *Scott* CP fixes two interaction parameters (g_x and Δg), leaving the third one free to assume any value ($\bar{g}$), while for a *regular* CP, even an infinitesimally close one, the composition alone does not fix any of the three parameters, yet after selecting a value for one of them the other two become determined.

3. Perturbation and Stability of Scott CPs

Conspicuous in Figure 3 is the narrow "neck" formed by the surface of constant φ. The displayed lines here *do not* intersect at a single point, as was the case with the iso-w_2 lines of the conic HODCP surfaces;[5] however, the presence of the neck suggests that, in the respective interval of $\bar{g}$, the critical value of w_2 is extremely sensitive to the variation of Δg and/or g_x. For a system with a trajectory passing through this region one would intuitively expect a critical line in the composition triangle oriented *across* the Scott line $w_2 = w_{2,S}$ rather than *along* it. This situation can be analyzed quantitatively by following the method outlined in the section 2.3 of ref 7.

By perturbing the values of critical variables, a Scott CP can be transformed into another CP, Scott or regular. Obviously not all perturbations will do that, only those that do not alter the zero value of the critical functions 5–7. The permitted perturbations thus have to satisfy the relations

$$\delta F_c \propto \delta w_2 - 3w_1^2\,\delta\xi^2 = 0 \tag{10}$$

$$\delta G_c \propto g_x\,\delta\varphi + \varphi\,\delta g_x = 0 \tag{11}$$

$$\delta H_c \propto \rho_1\rho_2\left[2\varphi\left(2\bar{g} - \frac{1}{\varphi_0}\right) - (\nu^2 + 3\mu^2)\right]\delta\xi^2 + r_1\Delta g\,\delta\varphi + r_1\varphi\,\delta\Delta g = 0 \tag{12}$$

where the last relation was rearranged by employing eq 10. The result is relatively simple since some terms drop out if the reference CP is of Scott type. These equations indicate that, to the first-order approximation, (i) the critical ξ^2 can be modified *only* by changing w_2, i.e., by a *horizontal* perturbation in the composition triangle, transforming a Scott CP into a regular one; (ii) g_x can be changed *only* by varying φ, i.e., by a perturbation *along* the Scott line that preserves the special character of such a CP; and (iii) Δg is affected by changes in both w_2 and φ.

The statement (i) is consistent with the fact that all Scott CPs are characterized by a constant w_2 *and* constant ξ^2 (cf. eq 1 and 8), and the point (ii) explains why the tangential vertical plane to the constant-φ surface at $w_2 = w_{2,S}$ in Figure 3 has to be parallel to the Δg axis.

Equation 12 combined with eq 10 predicts sensitivity of the partial derivative $\Delta\mathbf{g}_w \equiv (\partial\Delta g/\partial w_2)_\varphi$ at a Scott CP to the value of the mean polymer–solvent parameter $\bar{g}$ – a quantity that, so far, seemed to be immaterial.[1,4] Just as observed in Figure 3, the derivative $\Delta\mathbf{g}_w$ is positive for $\bar{g} < \bar{g}_{HE}$, negative for $\bar{g} > \bar{g}_{HE}$, and proportional in magnitude to the difference $|\bar{g} - \bar{g}_{HE}|$, where

$$2\bar{g}_{HE} = \frac{1}{\varphi_0} + \frac{1}{2\varphi}(\nu^2 + 3\mu^2) \tag{13}$$

Physically this means that, e.g., for $\bar{g} \ll \bar{g}_{HE}$, a relatively large increase in Δg is required to force a Scott CP off its line to a somewhat higher w_2. This fact then explains the extraordinary compositional "stability" of Scott CPs to the perturbation of g parameters as demonstrated numerically below, and to a degree it also justifies the original Scott's approximate formulation of his relations (1) and (2) with no regard to the relation (3). However, the situation is just the opposite around $\bar{g} = \bar{g}_{HE}$ where the derivative $\Delta\mathbf{g}_w$ becomes zero, indicating extremely high sensitivity of w_2 to the slightest perturbation of Δg and substantiating quantitatively the ideas outlined in the first paragraph of this section.

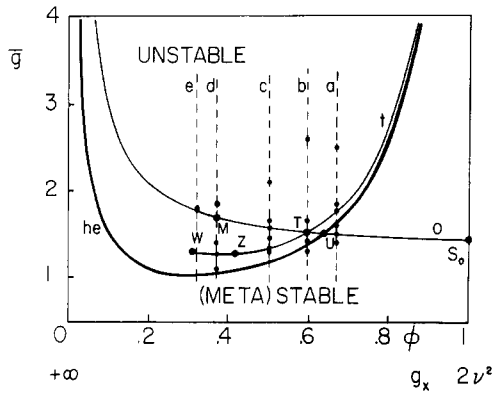

Figure 4. Critical point diagram for systems with Scott CPs ($r_1 = 2$, $r_2 = 5$), plotted in coordinates mean polymer–solvent interaction parameter $\bar{g}$ vs polymer concentration φ (or g_x of eq 9b): he, boundary of eq 13 separating (meta)stable Scott CPs below from the unstable ones above; t, locus of Scott CPs coexisting with two HODCPs, types 1 and 2 (eq 16); 0, locus of Scott CPs coexisting with a HODCP of type 0 (eq 17); the lettered points are identified in the text. Verticals a–e mark trajectories of systems discussed in Figures 6–10, with points defining the $\bar{g}$ levels of displayed spinodals.

There is another important consequence of the derivative $\Delta \mathbf{g}_w$ being zero: it means that at $\bar{g} = \bar{g}_{HE}$ the vertical locus of Scott CPs intersects two of its infinitesimally close neighbors. In Figure 3 this behavior is approximated by lines for $w_2 = 0.38$ and $w_2 = 0.40$ and their point of intersection HE on the Scott line. However, any intersection of two infinitesimally close lines in the g-space indicates simultaneous existence of two infinitesimally close CPs in the composition diagram, i.e., the presence of a double CP. It can be proven (see Appendix) that the point HE is indeed a heterogeneous double CP, but not a triple CP; hence, it will be referred to as the *Scott HEDCP*. Its presence has implications for the *stability* of Scott CPs: It is known that HEDCPs mark the boundary between thermodynamically (meta)stable and unstable CPs.[7-9] Thus all Scott CPs below the point HE of Figure 3 are (meta)stable while those above it are unstable. Figure 4 displays the entire Scott half-plane, compressed to a finite size by using φ instead of g_x as the abscissae axis; here again, $\bar{g}_{HE}$ of eq 13 (bold curve he) separates the (meta)stable Scott CPs *under* the curve from the unstable ones *above* it. At the interval ends the curve diverges, and it has a minimum with coordinates

$$(\varphi/\varphi_0)_{min} = [(\nu^2 + 3\mu^2)/2]^{1/2}$$

$$2(\bar{g}_{HE})_{min} = [1 + (\varphi/\varphi_0)_{min}]^2 \qquad (14)$$

In view of these findings, it is not quite correct to say that for a Scott CP the value of the mean solvent parameter $\bar{g}$ is unimportant: it determines whether the CP is physically meaningful or not. Only at $\bar{g} < (\bar{g}_{HE})_{min}$ is its (meta)stability guaranteed; at higher $\bar{g}$ values this has to be decided from eq 13.

4. Coexistence of Scott CPs with HODCPs

Under certain conditions, Scott CPs can coexist with HODCPs at the same temperature. In the composition triangle, the HODCPs have to be located on the borders of the three-valued region of the ξ^2-surface, i.e., on one of the linear segments 0, 1, or 2 connecting the binary CPs (see Figure 1). In the g-space, the locus of HODCPs belonging to a given segment is a portion of a biconical surface.[5] Figure 5 shows a projection into the base plane g_x,Δg of all three such surfaces, in the form of three bisectors with vertices V_i, one of 90° (0) and two of 45° (1,2). Note that only the upper hyperbolic surfaces H_i intersect

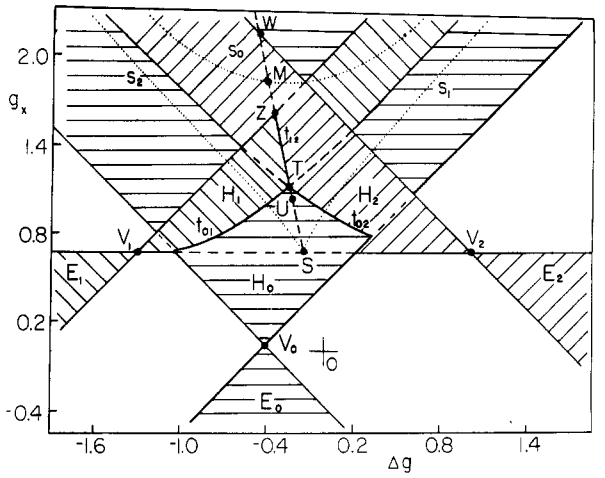

Figure 5. Two-dimensional projection of some features of the g-space onto the base plane g_x–Δg for the system $r_1 = 2$, $r_2 = 5$.[5] V_0, V_1, and V_2 are vertices of the three biconical HODCP surfaces, here projected into bisectors of 90° (0) and 45° (1 and 2). For $g_x > g_{x,min}$ (eq 4) surfaces partly overlap, forming three lines of intersection t_{ij}. Scott half-plane projects into t_{12}. Visibility as viewed from below (i.e., from negative $\bar{g}$) is indicated by full-dashed pattern of some lines and by the characteristic hatching. (···) Boundaries s_i between metastable hyperbolic and unstable elliptic regions, all located on "invisible" surfaces; T, system with three HODCPs; O, origin.

each other (lines t_{ij}), as well as the Scott half-plane projecting into t_{12}. On the other hand, the lower sectors E_i representing (meta)stable elliptic HODCPs come never even close to the Scott half-plane; this is consistent with the finding that closed-loop and polymer–polymer instabilities cannot coexist.[10] In the text below some quantitative criteria are developed for the coexistence of Scott CP with hyperbolic HODCPs, and the results are plotted in the Scott half-plane of Figure 4. It can be proven that the pattern of Figure 4 (i.e., the sequence $g_{x,W} > g_{x,M} > g_{x,Z} > g_{x,T} > g_{x,U}$) stays the same independent of r_1 and r_2, as long as $r_1 < r_2$. Thus the phase diagram development examined in this account is quite general.

It was noted recently[5] that the intersection line t_{12} satisfies the Scott ratio $g_x/\Delta g$ of eq 9c; in fact, even its starting point in Figure 5 (point S) is the same as for Scott CPs (cf. $g_{x,min}$ of eq 4). However, t_{12} ends at a finite value $g_{x,Z}$ (point Z) on the edge of type 1 conical section where

$$g_{x,Z} = g_{x,min}(1 + \rho_1) \qquad (15)$$

Thus a system with heteroparameters fitting eq 9c, with $g_{x,min} < g_x < g_{x,Z}$, and with $\bar{g}$ equal to $\bar{g}_t$ of the line of intersection t_{12} where

$$2\bar{g}_t = \frac{1}{\varphi_0} + \frac{1}{\varphi}(\nu^2 + \mu^2) \qquad (16)$$

should display in the composition diagram *simultaneously* two (meta)stable hyperbolic HODCPs (one each of types 1 and 2) *and* a Scott CP. (Equation 16 has been obtained from eq 15 and 27 of ref 5.) One can also say that any ternary phase diagram with the above two HODCPs possesses necessarily a Scott CP as well. It can be proven that all three CPs share the same total polymer concentration φ appearing in eq 16 (and fixed by g_x through eq 9b), although they obviously have to differ in w_2. They are located on a spinodal degenerated into a horizontal line. Furthermore, from comparison of eq 13 and 16, it follows that $\bar{g}_t \geq \bar{g}_{HE}$, indicating that this type of Scott CP is never thermodynamically stable. This is also apparent from Figure 4 where $\bar{g}_t$ of eq 16 is plotted as the locus t; in all instances it stays above the curve he.

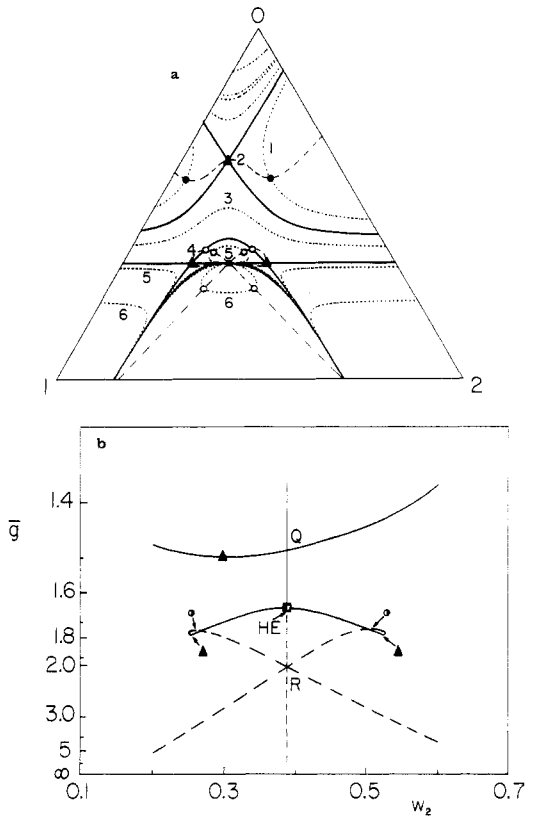

Figure 6. Model Scott system with trajectory a, $g_x \approx 0.9944$, $\Delta g \approx -0.2239$, and $\varphi_S = 0.67$. (▲) Hyperbolic HODCP. (a) Composition triangle projection. (■) Scott CPs. Regular single CPs: (●) (meta)stable; (○) unstable. (···) Spinodals for $\bar{g}$ values as follows: 1, 1.4; 2, 1.5013 $\approx \bar{g}_{HO}$; 3, 1.6; 4, 1.7763 $\approx \bar{g}_t$; 5, 1.8333; 6, 2.5. Spinodals associated with HODCPs are emphasized by full lines; (- - -) critical line (CL). (b) CL in expanded $\bar{g}$ vs w_2 coordinates: (—) stable; (- - -) unstable; (◑) HEDCP [not shown in (a)]; (◧) Scott HEDCP.

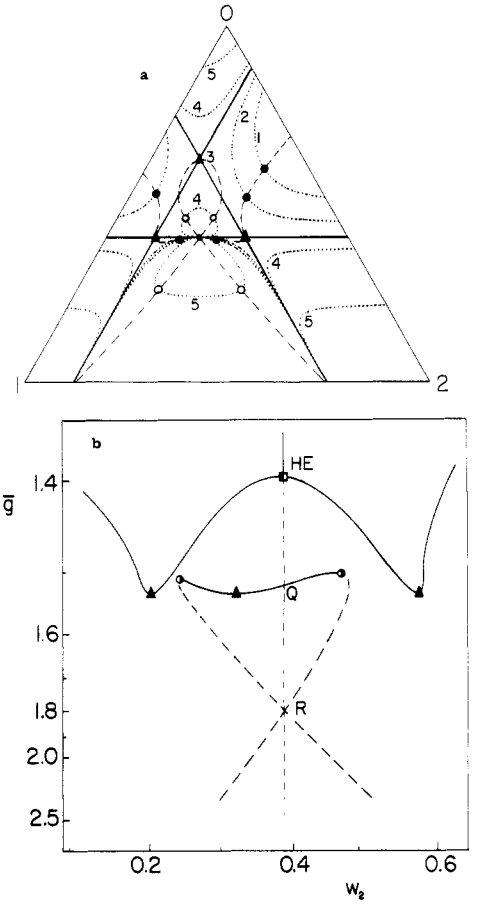

Figure 7. Scott system with trajectory b, $g_x \approx 1.1193$, $\Delta g = -0.2520$, and $\varphi_S \approx 0.5952$. Except as noted, the symbols are the same as in Figure 6. (a) $\bar{g}$ values for spinodals: 1, 1.3; 2, 1.42; 3, 1.5293 $\approx \bar{g}_{HO} \approx \bar{g}_t$; 4, 1.63; 5, 2.588. (b) CL in expanded $\bar{g}$ vs w_2 coordinates.

The Scott vertical half-plane also intersects the HODCP surface of type 0 at $\bar{g} = \bar{g}_{HO}$ given, by combination of eq 9b and 9c with the appropriate form of eq 15 of ref 5, as

$$2\bar{g}_{HO} = \frac{[\nu(\nu + 1) - \mu^2]^2}{\nu^2 - \varphi\mu^2} + \frac{\mu^2 + \nu^2}{\varphi} \qquad (17)$$

where φ specifies the polymer volume fraction at the Scott CP. Since the Scott line, eq 9c, of Figure 5 is fully contained within the 0 sector, it is apparent that this line of intersection *does not* end at a finite g_x value as was the case for t_{12}; other distinctions are that (i) in the composition space the Scott CP and its associated 0-type HODCP *do not* share even the same φ values and (ii) such Scott CPs can be (meta)stable, i.e., physically significant (see curve 0 in Figure 4).

Physical consequences of the above results are demonstrated in Figures 6–10 by tracing the development of critical and spinodal patterns in hypothetical Scott systems ($r_1 = 2$, $r_2 = 5$) with vertical trajectories, gradually shifting from low to high g_x values (dashed lines a–e in Figure 4). The condition of verticality guarantees a fixed composition for the Scott CPs, independent of temperature, making it easier to spot trends in the development of other phase-diagram features. All of these figures contain triangular composition diagrams with spinodals (···) plotted for $\bar{g}$ levels indicated by small dots in Figure 4. The asymptotic spinodals passing through the hyperbolic HODCPs are emphasized by full lines, and the critical lines (CLs) are drawn as dashed lines. In some cases also the temperature plots of CLs are shown, with full-dashed

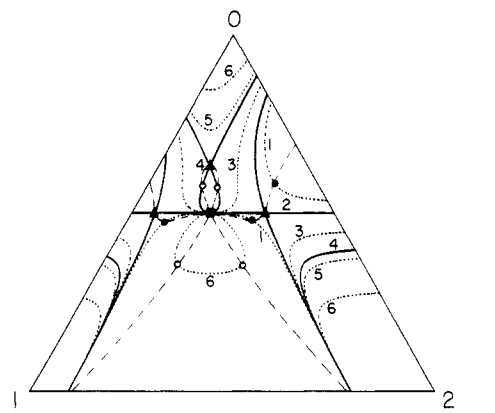

Figure 8. Scott system with trajectory c, $g_x \approx 1.3325$, $\Delta g = -0.3$, $\varphi_S = 0.5$, and $\bar{g}$ values as follows: 1, 1.3; 2, 1.35 = $\bar{g}_t$; 3, 1.45; 4, 1.5792 $\approx \bar{g}_{HO}$; 5, 1.652; 6, 2.1. Other notation is the same as in Figure 6.

pattern distinguishing their (meta)stable and unstable portions.

For the triplet of g's corresponding to the point S_0 of Figure 4, the Scott CP with $g_x = g_{x,min}$ is in the composition diagram at its bulk limit at $\varphi = 1$ (since the polymer incompatibility is too weak to force the miscibility gap into the triangle proper). For this marginal case, the associated hyperbolic HODCP of 0 type is on the linear segment 0 at $w_2 < w_{2,S}$, specifically at

$$w_2 = \frac{1 - \rho_1\rho_2\mu}{2\rho_2(\nu + \rho_1\rho_2\mu^2)} \qquad \varphi = \frac{\nu + \rho_1\rho_2\mu^2}{\nu(1 + \rho_1\rho_2\nu)} \qquad (18)$$

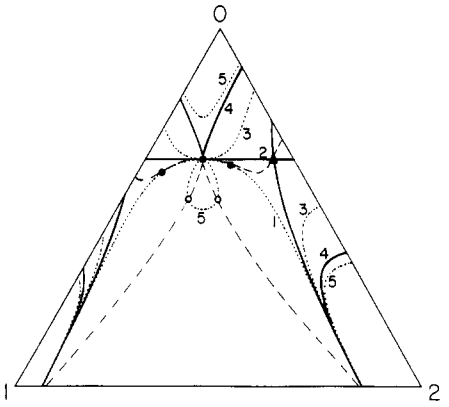

Figure 9. Scott system with trajectory d, $g_x \approx 1.8205$, $\Delta g \approx -0.4099$, $\varphi_S \approx 0.366$, and $\bar{g}$ values as follows: 1, 1.1; 2, 1.2668 $\approx \bar{g}_t$; 3, 1.4; 4, 1.6989 $\approx \bar{g}_{HO}$; 5, 1.80. Other notation is the same as in Figure 6.

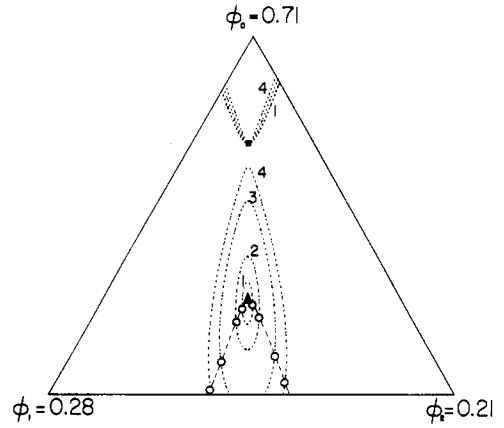

Figure 10. Magnified portion of the spinodal diagram for a Scott system with trajectory e, $g_x \approx 2.0820$, $\Delta g \approx 0.4687$, and $\varphi_S = 0.32$. (▲) Unstable elliptic HODCP for $\bar{g} \approx 1.7646$, surrounded by spinodals for $\bar{g}$ values as follows: 1, 1.7648; 2, 1.7656; 3, 1.7692; 4, 1.7729. Other notation is the same as in Figure 6.

and both of these CPs are (meta)stable. As the system's representative point then advances from S_0 along the line 0 (moving up from S of Figure 5), both CPs in the composition diagram shift along their respective loci toward higher w_2 and lower φ, maintaining the inequality $\varphi_{HODCP} < \varphi_S$, and $\bar{g}_{HO}$ keeps increasing. Simultaneously $\bar{g}_t$ of eq 16 drops to finite values (cf. t of Figure 4), producing on a different $\bar{g}$ level two (meta)stable HODCPs of types 1 and 2 coexisting with an unstable Scott CP.

This situation is illustrated in Figure 6a for a Scott system with the trajectory a of Figure 4. At low $\bar{g}$ (curve 1) the spinodal has three different branches, each penetrating into the triangle from one of its sides. While the Scott spinodal, based on 1–2 axis, is at first insensitive to the growing $\bar{g}$ (2 and 3 being hardly distinguishable from 1 in Figure 6a), the other two spinodals make contact at a hyperbolic HODCP, type 0 (2) and coalesce into one unstable region (3). Only as $\bar{g}$ approaches and exceeds $\bar{g}_{HE} \approx 1.6583$ where the Scott CP becomes unstable, the spinodal around it flattens, forms a horizontal at $\bar{g} = \bar{g}_t$, and changes the sign of its curvature. The spinodal with $\bar{g} = \bar{g}_t$ (4) thus represents a boundary between the common "closed" patterns 1–3 (the instability gap based on 1–2 axis closes at the Scott CP) and "open" patterns 5 and 6 (the gap spreads to the polymer–solvent axes 0–1 and 0–2). As expected, the Scott CP stays anchored at one spot for all temperatures. The "island" formed above the Scott CP (5) will typically be metastable, not stable, due to the coalesced miscibility gap expanding from its origins on 0–1 and 0–2 axes. For $\bar{g}$ growing even further the open pattern of Scott spinodals persists, and the island eventually flips around the Scott CP downward (6).

This system exhibits three distinct critical lines. In Figure 6a only two of them are apparent (dashed), with the third one being projected as a single Scott CP. A better display is afforded in coordinates $\bar{g}$ vs mixed-polymer composition w_2 (Figure 6b) where the vertical Scott CL is clearly seen. Only one of the CLs (the upper one in both diagrams) is stable all along, carrying the HODCP type 0 (spinodal 2) at its minimum.[11] The lower CL displays a complex, almost symmetrical pattern with three maxima and two minima. It starts at $\varphi \to 1$ and $T \to 0$ ($\bar{g} \to +\infty$) as two unstable branches pointing against one another. Each branch eventually reaches its own maximum occupied by a HEDCP, where it becomes stable, and then turns downward, reverses smoothly its direction relative to w_2, passes through a minimum carrying a stable HODCP (spinodal 4), and rises toward the Scott CP (□) where both branches smoothly join in their common absolute maximum. This point is also a HEDCP separating the vertical Scott CL into a stable upper and an unstable lower part. Its role will be detailed later; here let us just note that HE marks the only instance where the Scott CL genuinely interacts with another CL. The point Q is no true intersection as can be seen from the composition projection in Figure 6a or by comparison of the ξ^2 values of both curves (the upper transverse CL runs on the ξ^2-surfaces 1 and 2, while the Scott CL lies in the midst of the ξ^2-surface 0). The trivial criterion fails in the case of point R where three CLs cross each other in both projections, thus giving an impression of a genuine point of intersection. Yet, ξ^2 values show again that the three seemingly overlapping CPs are in fact each different: the ascending line of Figure 6b lies in the ξ^2-surface 1, the descending line in 2, and the Scott vertical in the surface 0. This case well illustrates the importance of the parameter ξ^2; without it, the three CPs would be indistinguishable.

At the point U (Figures 4 and 5), the lines of intersection of the Scott vertical half-plane with the HEDCP surface and with the 0-type HODCP surface (curves he and 0, respectively, of Figure 4) cross one another; i.e., $\bar{g}_{HO}$ of eq 17 becomes equal to $\bar{g}_{HE}$ of eq 13; this happens for $g_x = g_{x,U}$ where

$$g_{x,U} = 2\nu^2 + (8\nu^2 + \kappa^2)^{1/2} - \kappa \qquad (19)$$

and

$$\kappa = 3(\nu^2 - \mu^2) + 4\nu$$

Physical consequence is that any Scott CP with $g_x > g_{x,U}$ (or $\varphi < \varphi_U$), coexisting with a hyperbolic (meta)stable HODCP of the 0th type, is thermodynamically *unstable*. Some of these cases are displayed in Figures 7–9.

With the representative point sliding further up along t_{12} of Figure 5, the spinodal at $\bar{g}_t$ (analogue of 4 of Figure 6a) changes: the horizontal shifts toward lower φ, and the arch above it becomes more pointed and approaches the composition of HODCP, type 0. Simultaneously, the lower part of spinodal for $\bar{g}_{HO}$ (cf. 2 of Figure 6a) conforms more and more to the shape of $\bar{g}_t$ spinodal, until at T both curves merge in their entirety. In this unique system with parameters characterized by eq 29 and 30 of ref 5, all three HODCPs coexist, at the same temperature, located at the vertices of a triangle formed by three linear spinodals parallel to the composition triangle sides (Figure 7a, trajectory b of Figure 4).[5] This symmetrical case also represents a boundary between systems with polymer–solvent miscibility gaps merging first together in a HODCP on segment 0 [leading to a metastable island formation

(Figure 6a)] and systems where each of these gaps merge first with the Scott unstable region (Figures 8–10, trajectories c–e). The (meta)stable "peninsula" thus created in the latter case (curve 3 of Figure 8) extends all the way to the solvent vertex, and it is sealed off only at a higher $\bar{g} = \bar{g}_{HO}$ via an HODCP of type 0 (curve 4).

The CL pattern for systems b and c is also different from that for a: the upper CL of Figure 6a is now deflected down and runs through HODCPs types 1 and 2, instead of 0 (i.e., it also visits the ξ^2-surface 0), while the complex loop system of the lower CL is transformed into a simple vertically oriented loop passing through HODCP type 0 (i.e., this CL now runs exclusively on ξ^2-surfaces 1 and 2). Consistent changes are seen in $\bar{g}$ plots (cf. Figures 6b and 7b). The switch in CL pattern seems to proceed via merging of two HEDCPs; its analysis, however, is beyond the scope of this paper and will be presented in the future.

As the system's trajectory moves through the point Z, the left HODCP of Figure 8 (type 1) exits through the binary critical point CP_{01}. Consequently, systems with $g_{x,W} > g_x > g_{x,Z}$ possess only two HODCPs (types 0 and 2, each at a different temperature), and the pairs of spinodal branches originating from 0–1 instability always diverge from one another (left portions of curves 2–5 of Figure 9). Note that with the HODCP type 1 gone, the switch between the closed and open patterns of Scott spinodals relative to 0–1 axis now occurs at $\bar{g}_{CP_{01}}$ rather than at $\bar{g}_t$. A particular situation arises at the point M (trajectory d) marking the intersection of the Scott half-plane with the boundary line s_0 of Figure 5. Recall that s_0 separates hyperbolic meta(stable) HODCPs of type 0 (below) from elliptic unstable ones (above), and HODCPs on this boundary should also acquire characteristics of HEDCPs.[5] The conditions for the system corresponding to the point M can be derived from the equation for the boundary s_0, eq 19b of ref 5. It turns out that in the composition diagram of such a system the Scott CP and the 0-type HODCP, each traveling on its own locus, have just overlapped (■ in Figure 9) and share almost all of their characteristics

$$\varphi = \nu/(1+\nu) \qquad g_{x,M} = 2\nu(1+\nu)$$

$$\Delta g_M = -2\mu(1+\nu) \quad 2\bar{g}_M = (\nu+1)(2\nu+1) \tag{20a}$$

with w_2 given by eq 1. Yet it cannot be said that this is a genuine overlap since the two CPs are moving on two different ξ^2-surfaces (the Scott CP in the midst of surface 0, the HODCP on the weld of surfaces 1 and 2); hence they differ in their ξ^2 values ($-\rho_1/\rho_2$ and $+\rho_1/\rho_2$, respectively).

The 0-type HODCP here indeed acquires characteristics of an HEDCP as can be shown by substitution of eq 20a into the HEDCP criterion, eq 9 of ref 7, using $\xi^2 = +\rho_1/\rho_2$. As explained earlier (Figure 13 of ref 5), the loop-terminated asymptotic spinodal of the hyperbolic HODCP, type 0 (curve 4 of Figure 8), here transforms into a cusp-forming curve (4 of Figure 9) contacted from the opposite side by the CL. Also passing through this point is the horizontal spinodal for $\bar{g} = \bar{g}_t$ carrying a HODCP of type 2, albeit at a different temperature (curve 2).

With the representative point moving past the point M of Figure 5, the 0-type HODCP becomes of unstable elliptic type, sliding on the segment 0 to w_2 values higher than $w_{2,S}$, while the coexisting unstable Scott CP continues moving toward the solvent vertex 0. The upper bound on w_2 of the elliptic HODCP is $w_{2,max} = {}^1/_2$; it would be achieved in a somewhat unphysical limiting case of $g_x \to +\infty$, $\bar{g} \to +\infty$, $\varphi_S \to 0$. The elliptic nature of these HODCPs is illustrated in Figure 10 for a system with trajectory e of Figure 4. All CPs displayed in this magnified portion of the composition diagram are thermodynamically unstable. Correspondingly, the phases turn out to be metastable *inside* the loops and unstable *outside*, contrary to the usual arrangement.[5]

Finally, in a system mapped onto W of Figures 4 and 5, where

$$g_{x,W} = g_{x,min}(1+\rho_2) \tag{20b}$$

also the hyperbolic HODCP of type 2 exits from the composition triangle through the side 0–2. The phase diagram then becomes dominated by the Scott instability, which, with increasing $\bar{g}$, grows two "bumps" that penetrate into the polymer–solvent axes 0–1 and 0–2, leaving only the vertex regions (meta)stable.

5. Stability and Perturbation of Scott Critical Lines

In order to keep the spinodal diagrams simple, the examples above were computed for systems with vertical trajectories. In this section a more realistic choice is examined, with all three interaction parameters following the relation of the type

$$g = \alpha + (\beta/T) \tag{21}$$

where α and β are constants. In the interaction space, such a system is represented by a *linear* trajectory starting at the point $\bar{\alpha}$, $\Delta\alpha$, α_x for $T \to \infty$ and extending to infinity for $T \to 0$ in the direction $d\bar{g}:d\Delta g:dg_x = \bar{\beta}:\Delta\beta:\beta_x$ (see Figure 2).

From quasi-binary systems, one is accustomed to a single CL running *across* the composition triangle from CP_{01} to CP_{02} (upper CL in Figure 6a). For a long time it has been clear, however, that this could not be the only option in ternary systems proper. The existence of the binary CP_{12} alone suggests that some CL should connect there, and Scott's analysis of CPs[1] left no doubt about the nature of such a CL (s of Figure 1). This fact is also documented in Figures 6–9. With more than one CL crossing the composition space, an interesting question arises as to their mutual interaction: Do they genuinely cross at a point of intersection? What is the nature of such a point? Is it perhaps a multiple CP?

In this account only the interaction between a Scott CL and another CL will be pursued; the general case will be discussed elsewhere. We have seen already in some cases (points Q and R of Figures 6b and 7b) that, in fact, an apparent "intersection" may not be genuine and falls apart when the CL is projected into another space (composition triangle or ξ^2-surface). However, the point HE, intuitively suspected of being a true "crossing" point in section 3, passes the projection test and seems to be the only point of true interaction between the CLs. Insight into its nature can be gained by examining the slopes of CL at a Scott CP, $(d\varphi/dw_2)_S$ and $(dT/dw_2)_S$. The composition slope can be derived from eq 12 whose differential $\delta\xi^2$ is substituted from eq 10, and $\delta\Delta g$ put equal to $\Delta\beta\delta g_x/\beta_x$ (cf. eq 21) where δg_x is given by eq 11. The result is

$$\left(\frac{d\varphi}{dw_2}\right)_S = 4\varphi^2\beta_x(\rho_1+\rho_2)\frac{\bar{g}-\bar{g}_{HE}}{3(\mu\beta_x+\nu\Delta\beta)} \tag{22a}$$

where $\bar{g}_{HE}$ is defined by eq 13. The temperature slope can then be written, e.g., as

$$\left(\frac{dT}{dw_2}\right)_S = \frac{2\nu^2T^2}{\beta_x\varphi^2}\left(\frac{d\varphi}{dw_2}\right)_S \tag{22b}$$

An important factor for further considerations is the system's degree of adherence to the condition 9c for a Scott CP over a range of temperatures. In order to better com-

Table I
Ranges of Definition for Scott CLs of SSS with $g_x = \alpha_x + \beta_x/T$[a]

φ	$\alpha_x > 0, \beta_x > 0$		$\alpha_x > 0, \beta_x < 0$	$\alpha_x < 0, \beta_x > 0$
	$\mathcal{T} < 1$	$\mathcal{T} > 1$	$\mathcal{T} > 1$	
0	0	0		0
$\mathcal{T}^{-1}$	↓	↓ ∞	∞ ↓	↓
1	$\mathcal{J}$		$\mathcal{J}$	$\mathcal{J}$

[a] The table gives the temperatures T associated with the polymer volume fractions φ. Definition of symbols: $\mathcal{T} = \alpha_x/2\nu^2$, $\mathcal{J} = \beta_x/(2\nu^2 - \alpha_x)$.

prehend the behavior of real systems, it is useful to introduce the concept of a *strictly Scott system* (SSS), which would comply with the criterion 9c at *all* temperatures. From eq 21, this imposes severely restrictive conditions on the temperature coefficients

$$\mu\alpha_x = -\nu\Delta\alpha \qquad \mu\beta_x = -\nu\Delta\beta \tag{23}$$

which force the entire trajectory into the Scott vertical half-plane $g_x/\Delta g = -\nu/\mu$. Obviously, the model systems displayed in Figures 6–10 belong to this category. While very few real systems, if any, would satisfy such a requirement, this model is useful as an asymptotic frame of reference that can be more or less approached by real systems.

Much more common should be the case where the system's trajectory merely intersects the Scott half-plane. Then the condition 9c is *exactly* satisfied only at *one* particular temperature (call it Scott temperature)

$$T_S = -(\nu\Delta\beta + \mu\beta_x)/(\nu\Delta\alpha + \mu\alpha_x) \tag{24}$$

while in the temperature interval around T_S the compliance with 9c is only *approximate*. Another variation could be a trajectory with *no* intersection yet situated at least partially in the proximity of the Scott half-plane. In the spirit of the original proposition written in approximate terms,[1] these systems will be referred to as (plain) *Scott systems*. It should be clear, however, that more appropriately one should speak of *Scott behavior* or *Scott temperature range* since even an approximate compliance with his criteria is typically guaranteed only at some temperatures, until the trajectory strays too far from the Scott half-plane.

The term *Scott critical point*, on the other hand, shall be used only for a CP satisfying the relations 9 *exactly*; for the most part of real systems this would happen only at T_S of eq 24. Critical points satisfying these criteria only loosely shall be called *perturbed* Scott CPs.

5.1. Strictly Scott Systems. Leaving aside the degenerate case of $\beta_x = \Delta\beta = 0$ with a single Scott CP for all temperatures, the composition diagram of a SSS should display a *line* of Scott CPs of constant w_2, while in the temperature coordinates T vs w_2, it should be a vertical positioned at $w_{2,S}$. The T vs φ calibration of the Scott CL is provided by combination of eq 9b and 21

$$\varphi = 2\nu^2 T/(\alpha_x T + \beta_x) \tag{25}$$

The Scott CL may not be defined in its entirety as shown in Figure 1; its ranges of definition are shown in Table I, assuming literal application of the temperature function 21 over the entire interval $0 < T < \infty$. In summary:

(i) No Scott CPs can exist for $\beta_x < 0$ if also $\alpha_x < 2\nu^2$.

(ii) They can exist in the entire concentration interval $0 < \varphi < 1$ only if $\beta_x > 0$ and $\alpha_x < 2\nu^2$.

(iii) In the remaining case of $\alpha_x > 2\nu^2$ the Scott CL *ends* within the composition triangle, short of $\varphi = 1$ (for $\beta_x > 0$) or short of $\varphi = 0$ (for $\beta_x < 0$). Its continuation would carry unphysical negative temperatures.

(iv) If they exist at all, the exits of the CL through the solvent vertex ($\varphi = 0$) and through the polymer 1–polymer 2 critical point CP_{12} ($\varphi = 1$) occur at temperatures $T = 0$ and $T = \beta_x/(2\nu^2 - \alpha_x)$, respectively.

(v) The effect of temperature depends on the sign of β_x: with growing T the critical concentration φ may increase (if $\beta_x > 0$) or decrease (if $\beta_x < 0$).

Note that the trivial divergence of the Scott CL slopes is reflected in eq 22a and 22b where both derivatives grow to infinity because of the satisfied condition 23 for β's. There can be only one exception to this scenario: at the Scott HEDCP ($\bar{g} = \bar{g}_{HE}$), the formulas 22a,b become of 0/0 type, i.e., indeterminate, and the slopes may be finite, indicating, this time in quantitative terms, the possible presence of a transverse CL. The coordinates of this crossing point, φ_{HE} and T_{HE}, are given by the point of intersection of the he curve of Figure 4 with the system's trajectory.[12] The result depends only on polymer chain lengths and the temperature coefficients of interaction parameters. The polymer concentration φ_{HE} is obtained from a quadratic equation as

$$\varphi_{HE} = \Xi \pm (\Xi^2 - 2\Lambda/\Gamma)^{1/2} \tag{26}$$

where

$$\Lambda = \beta_x(\nu^2 + 3\mu^2) - 8\bar{\beta}\nu^2 \qquad \Gamma = 8(\bar{\alpha}\beta_x - \alpha_x\bar{\beta})$$

$$\Xi = \tfrac{1}{2} + \frac{\Lambda - 2\beta_x}{\Gamma}$$

and the temperature T_{HE} follows from eq 13 and 21. The composition slope of the CL at this point can be evaluated, for instance, by expanding the three differential equations 10–12 to the second order and solving them, with the result

$$\left(\frac{d\varphi}{dw_2}\right)_{HE} = \frac{\mu\nu\varphi}{\Lambda/2\beta_x - (\varphi/\varphi_0)^2} \tag{27}$$

whereas the temperature slope can be calculated from eq 22b as usual.

Because of the physical implications of the curve he of Figure 4, systems with trajectories *tangent* to it play an important role: they form the boundary between systems whose entire Scott CL is (meta)stable and systems whose Scott CL is partly unstable. The condition for this borderline case is the existence of a double root of eq 26; i.e., $\Xi^2 = 2\Lambda/\Gamma$ or in a more elementary form

$$|\Gamma|^{1/2} = 2|\beta_x|^{1/2} + (2|\Lambda|)^{1/2} \tag{28}$$

where *all three* quantities, β_x, Γ, and Λ, have to be *of the same sign*; and the polymer concentration at which the instability originates is

$$(\varphi_{HE})_{1,2} = \Xi = 1 - 2(\beta_x/\Gamma)^{1/2} \tag{29}$$

The requirement of T_{HE} and φ_{HE} being physically meaningful imposes two additional inequalities on the relevant variables:

$$(\beta_x/\Gamma)^{1/2} < \tfrac{1}{2} \tag{30a}$$

$$2(\beta_x/\Gamma)^{1/2} > (\alpha_x - 2\nu^2)/\alpha_x \qquad \text{if } \alpha_x > 2\nu^2 \tag{30b}$$

For fixed r_1 and r_2, the tangent condition thus leaves the system's parameters with 3 degrees of freedom. To generate such a case, one might, for instance, choose the point of contact φ_{HE} and the coefficient β_x, compute Γ from eq 29 and Λ from eq 28, then choose α_x consistent with the above restrictions, and obtain the remaining $\bar{\beta}$ and $\bar{\alpha}$ from

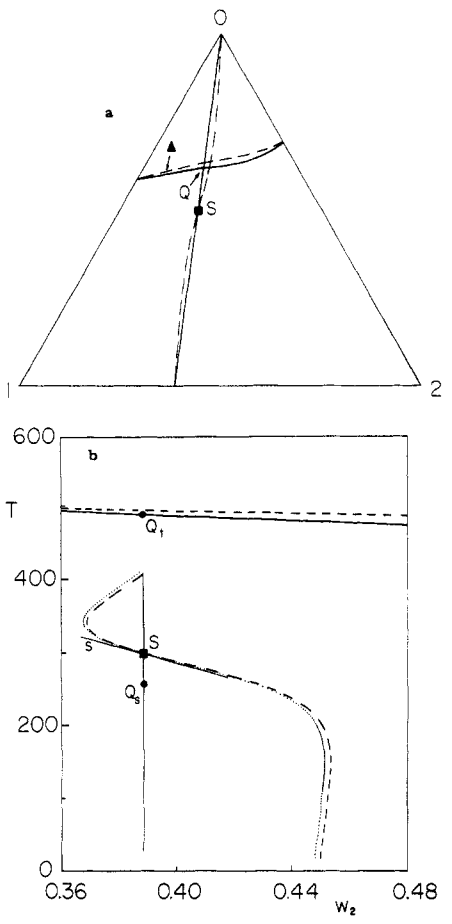

Figure 11. Critical lines, all (meta)stable, for a system with no Scott HEDCP: (—) SSS with $\bar{\alpha} = 2$, $\bar{\beta} = -336$, $\Delta\alpha \approx 0.27018$, $\Delta\beta \approx -171.11$, $\alpha_x = -1.2$, $\beta_x = 760$; (- - -) perturbed Scott system with modified variables $\Delta\alpha = -0.225$, $\Delta\beta = -22.5$; S Scott CP at $T_S = 300$ K (eq 24). (a) Composition triangle plot: (▲) HODCP type 0 in the perturbed system. (b) Magnified temperature plot: (···) result of the perturbation theory, eq 31 and 32; *s* slope to the perturbed Scott CL at S (eq 22).

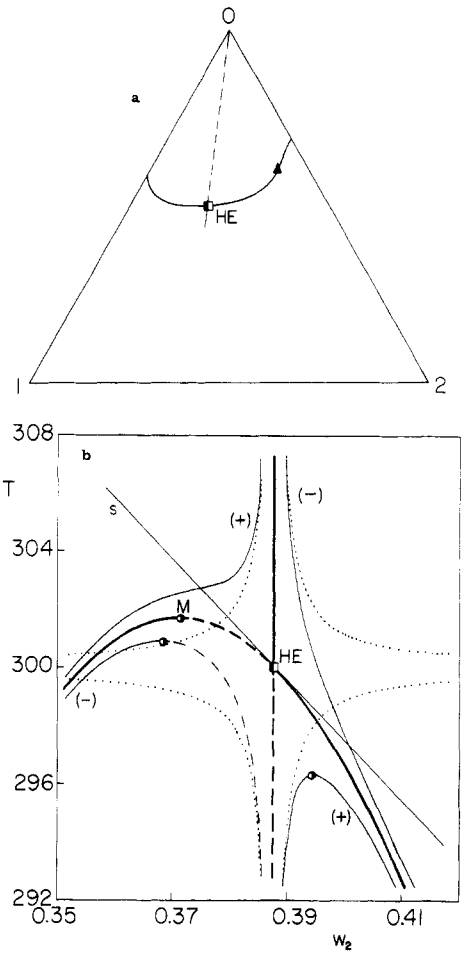

Figure 12. Critical lines for a system with one Scott HEDCP (HE). Unstable portions are drawn as dashed lines. SSS parameters are $\bar{\alpha} \approx 1.1627$, $\bar{\beta} \approx 8.7490$, $\Delta\alpha \approx 0.26906$, $\Delta\beta \approx 9.2812$, $\alpha_x \approx 1.1950$, $\beta_x \approx 41.223$. (a) Full composition plot for the SSS: (▲) HODCP type 2. (b) Magnified temperature plot of the region around HE: (◑) regular HEDCP [not shown in (a)]; (—) SSS; (+),(−) Scott systems with relative perturbations of $\delta\Delta g/\Delta g = \pm 0.01\%$; (···) prediction of the perturbation theory; *s* slope to the transverse CL at the Scott HEDCP for the SSS (eq 27).

definitions of Λ and Γ, respectively.

The condition for the Scott CL being (meta)stable all along (i.e., for eq 26 having no real solutions) is then $|\Gamma|^{1/2}$ < right-hand side of eq 28. On the other hand, if $|\Gamma|^{1/2}$ > right-hand side of eq 28 or if any of the sign conditions attached to eq 28 is not satisfied, this equation has real solutions, and the CL is partly unstable. An example of CLs for the former case is drawn as full lines in Figure 11. Note that the "vertical" Scott CL and the "transverse" CL do not share any common points; the apparent intersection Q ($w_2 = w_{2,S} \approx 0.3874$, $\varphi \approx 0.3689$) in Figure 11a turns out to be an overlap of two different points, as becomes apparent from the temperature plot in Figure 11b (a Scott CP Q_S with $T \approx 258.4$ K, given by eq 9b and 21, and its counterpart Q_t on the transverse CL with $T \approx 490.5$ K). In fact, in this particular case the Scott CL never reaches the temperature of Q_t; it ends at $T \approx 407.2$ K where the Scott CP exits the composition triangle via CP_{12} at $\varphi = 1$. Hence, the point Q of Figure 11a constitutes no HEDCP, and the Scott CL is indeed (meta)stable in its entirety.

A SSS with *one* physically significant Scott HEDCP at $\varphi_{HE} = 0.5$ and $T_{HE} = 300$ K is shown in bold lines in Figure 12. (The other solution of eq 26 was chosen to be outside the triangular limits at $\varphi_{HE} = -0.1$.) The diagram consists again of two CLs, with the Scott CL being (meta)stable only in a narrow volume fraction interval $^1/_2 < \varphi < 0.5575$ (Figure 12a). The temperature plot of the transverse CL of Figure 12a displays one HODCP minimum ($w_2 \approx 0.811$, $\varphi \approx 0.393$), in addition to a regular HEDCP maximum M close to the Scott composition w_{2S}. Only the latter portion is detailed in Figure 12b. The interaction parameters for this system have been determined one after another (no need for trial and error calculation) from the sequence of eq 26, 27, 22b, and 9b, to yield at the above specified point HE a relatively high, conspicuous slope of $(dT/dw_2)_{HE} = -200$ K. The hand-drawn slope of this magnitude fits very well the computer-plotted CL, which attests to the validity of eq 27. In comparison to the previous case, an important difference is that the point HE in Figure 12 is now genuinely common to both CLs: it stays preserved as such in both projections (a and b), and ξ^2 along the transverse CL at HE approaches $-\rho_1/\rho_2$, the value characteristic of Scott CPs. Furthermore, as they pass through HE, the CLs switch their stabilities whereas no such change has occurred with "noninteracting" CLs of Figure 11.

When the SSS trajectory in Figure 4 intersects the he curve twice, the interacting CL forms a closed loop with two Scott HEDCPs on it (HE_1 and HE_2). For the system of Figure 13 they are given by eq 26 as $\varphi_{HE} \approx 0.6266$ and 0.7359. Note that the apparent intersection of the upper transverse CL with the Scott CL in Figure 13a is again fictitious, as it was in Figure 11; the former line runs entirely on ξ^2 surfaces 1 and 2 as is apparent from the existence of its HODCP type 0, while the Scott CL is on the

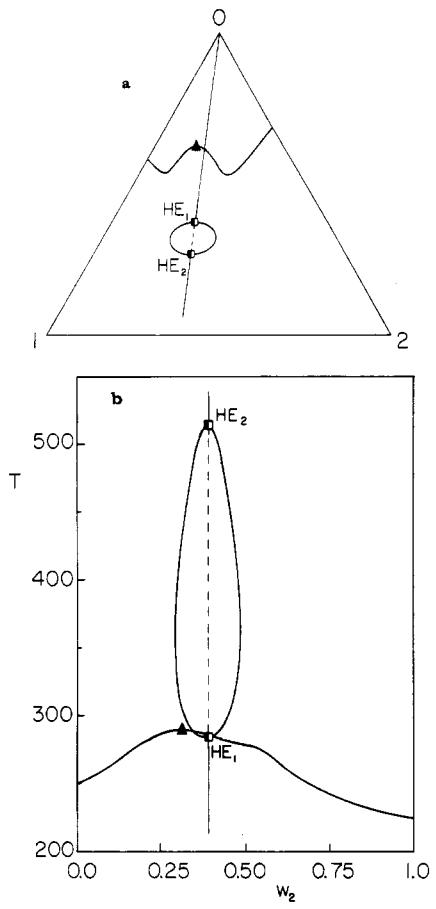

Figure 13. Critical lines of a SSS with two Scott HEDCPs (HE_1, HE_2). Parameters are $\bar{\alpha} \approx 2.6782$, $\bar{\beta} \approx -336.49$, $\Delta\alpha = -0.16$, $\Delta\beta \approx -22.515$, $\alpha_x \approx 0.7108$, $\beta_x = 100$: (---) unstable portions; (▲) HODCP type 0. Regular HEDCPs (temperature extrema) and unstable portions of the loop cannot be distinguished on this scale. (a) Composition plot; (b) temperature plot.

surface 0 as always. The transverse CL is entirely (meta)stable (cf. Figure 13b), while the Scott CL is only partly so: its portion between HE_1 and HE_2 passing through the loop is unstable, and it reaches only to $\varphi \approx 0.9373$ where $T \to \infty$. Also small portions of the loop itself between its temperature extrema (regular HEDCPs, not shown) and Scott HEDCPs (HE_1 and HE_2) are unstable, although this range is too small to be displayed in the full-scale Figure 13.

The above account of the CL patterns is logical and consistent except for one puzzling point: it is the nonzero slopes at HE predicted by eq 27 and 22b and displayed exemplarily in Figure 12b. Recall that HE should be a heterogeneous double CP (cf. the Appendix), which is normally manifested by an *extremum* of the CL $T(w_2)$.[7,8] No such extremum is evident from Figure 12b. This unusual behavior is due to the singular nature of Scott CPs and can be best clarified by examining slightly modified systems having the condition 23 somewhat relaxed, i.e., in our terminology, (plain) Scott systems.

5.2. Scott Systems. When the Scott condition 9c is met at only one temperature, $T = T_S$ (cf. eq 24), the "ideal" CL of SSS is modified. An interesting question arises whether such a shift in CL can be predicted by some simple method, e.g., by a first-order perturbation theory. While an obvious basis for its development might seem to be the genuine Scott CP (S) associated with the above temperature T_S, it would be a poor choice. This becomes apparent from the top-view projection of the system's trajectory (dashed line) and Scott half-plane (full line) in

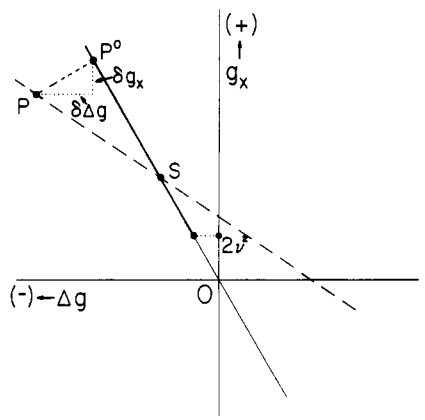

Figure 14. Two-dimensional projection of the Scott half-plane (—) and of the trajectory of a Scott system (---): S, Scott CP; P, perturbed system at certain temperature; P°, its "image" in the Scott half-plane.

Figure 14. The line representing the latter passes through the origin of $g_x,\Delta g$ plane with the ideal slope of $g_x/\Delta g = -\nu/\mu$, whereas the system's trajectory attains this ratio only at the intersection point S. It is evident that for any temperature of the perturbed system (here specified by the point P) the geometrically closest SSS lies on a perpendicular to the half-plane (point P°). For this reason we prefer to base the perturbation for each temperature at a different hypothetical Scott point. In other words, as the reference for the trajectory of the perturbed system serves its orthogonal projection into the Scott half-plane, with $\bar{g}^\circ \equiv \bar{g}$. All perturbations $\delta x \equiv x - x^\circ$ turn out to be linear functions of the system's distance from the Scott point S. By strictly geometrical considerations, the interaction perturbations in the reduced form are given simply by

$$(\nu^2 + \mu^2)\delta g_x/\mu = (\nu^2 + \mu^2)\delta\Delta g/\nu = \mu(g_x - g_{x,S}) + \nu(\Delta g - \Delta g_S) = (\mu\beta_x + \nu\Delta\beta)(T_S - T)/TT_S \quad (31)$$

while perturbations of state variables are (cf. eq 10–12)

$$\delta\varphi = \frac{-\varphi^\circ}{g_x^\circ}\,\delta g_x \qquad \delta\xi^2 = {}^4/_3 r_1\nu^2\,\delta w_2$$

$$\delta w_2 = \frac{3\nu^{-2}}{8\rho_1\rho_2}\,\frac{r_2 + r_1}{r_2 - r_1}\,\frac{\delta g_x}{(\bar{g}_{HE}^\circ - \bar{g})} \quad (32)$$

where $\bar{g}_{HE}^\circ$ is evaluated from eq 13 using $\varphi = \varphi^\circ$. Note that the coordinates $g_{x,S}$ and Δg_S can be omitted from eq 31 since they have to satisfy eq 9c.

Thus for any point P ($g_x,\Delta g$), its interaction perturbations δg_x and $\delta\Delta g$ and its reference state P° ($g_x^\circ,\Delta g^\circ$) can be determined from eq 31, the unperturbed values of other parameters calculated from the Scott equations 1, 8, and 9b, and their perturbed values from eq 32. One possible measure of the intensity of perturbation is the geometrical distance $\overline{PP^\circ} \equiv \delta g = (\delta g_x^2 + \delta\Delta g^2)^{1/2}$, which equals (the right-hand side of eq 31)$/(\nu^2 + \mu^2)^{1/2}$.

Most important for the appearance of the CL diagram is the variation δw_2 deflecting the "vertical" Scott line left or right from its ideal course. The above expressions immediately reveal several points about this quantity: (1) *Only* at the Scott temperature T_S are all perturbations zero, i.e., the perturbed CL intersects the ideal CL. (2) As $\bar{g} \to \bar{g}_{HE}^\circ$ (i.e., as the trajectory of the reference system in the Scott half-plane crosses he of Figure 4), δw_2 diverges left or right, leading to a discontinuity of the first-order estimate of the CL at HE°. (3) The polarities of perturbation δw_2 below and above HE° are opposite. (4) The sign

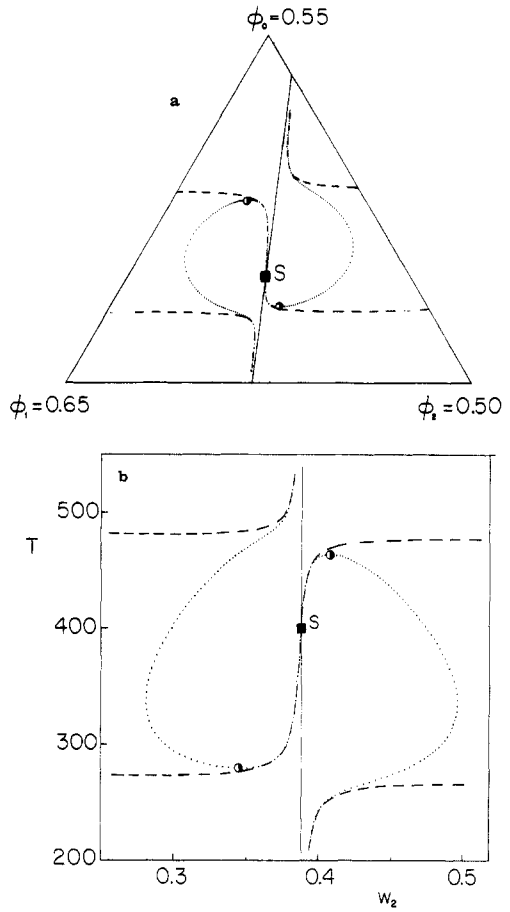

Figure 15. Magnified plots of the CL loop for a perturbed Scott system derived from the SSS of Figure 13: modified parameters $\alpha_x \approx 0.6753$, $\beta_x \approx 114.2$; S, Scott CP at $T = 400$ K; (●) HEDCP; (···) exact calculation; (- - -) perturbation theory.

of δw_2 also switches with changing polarity of perturbations δg_x and $\delta\Delta g$. (Note that because of eq 31 both of the latter quantities are of the same sign.)

The performance of the first-order perturbation theory and the validity of the above conclusions are illustrated in Figures 11, 12, and 15. As explained above, there is no interaction between the two skew CLs of Figure 11; hence, each behaves independently of the other. In the original SSS only $\Delta\alpha$ and $\Delta\beta$ have been varied by −183% and +87%, respectively, to produce a system with the Scott temperature of 300 K. For instance, at $T = 100$ K, this translates into a perturbation of $\delta g \approx 0.967$, with relative changes in g_x and Δg being +3.4% and −67.7% (cf. eq 31). In spite of this relatively large perturbation, the shift in CLs is modest (the dashed lines in Figure 11) and its approximation for the Scott CL by the first-order perturbation theory very good: any distinction between the two at all can be observed only on the enlarged scale of Figure 11b (dotted). The slope $(dT/dw_2)_S \approx -1062$ calculated from eq 22 fits the perturbed CL at S very well.

The singular character of a true point of "intersection" HE is confirmed by Figure 12b. The course of CLs in the neighborhood of HE is extremely sensitive to the perturbation of Scott conditions: the lines represent systems with $\Delta\alpha$ and $\Delta\beta$ (hence also Δg), deviating a mere +0.01% [curve (+)] and −0.01% [curve (−)] from the Scott condition 9c, yet the CLs are markedly modified on the employed scale. Furthermore, the discontinuous pattern of perturbed lines indicates that the CLs of a SSS have to be discontinuous at HE as well. Thus, they should not be viewed as a vertical and a transverse CL intersecting one another. Rather the transverse CL turns at HE into a vertical one, and vice versa, with the curvature of the turn growing to infinity (hence the indeterminacy of the simple slope expression 22a). Note that in a SSS it is impossible to decide whether, e.g., the left transverse CL turns up or down since however small the perturbation is, its sign change turns the outcome over.

This interpretation also clarifies the above alluded-to puzzle about the HEDCP character of the point HE and yields a consistent picture of stabilities of CLs. If the CLs of the SSS in Figure 12b are viewed as the left one turning up and the right one dropping down at w_{2S}, then the point HE indeed represents two mutually touching infinitely sharp extrema (i.e., HEDCPs), one minimum and one maximum, the former one separating the left descending unstable portion from the upper (meta)stable vertical and the latter one dividing the unstable lower vertical from the (meta)stable right portion. Note that the displayed perturbation of $\delta\Delta g/\Delta g = +0.01\%$ is large enough to make the former minimum disappear together with the regular HEDCP maximum M, via a triple CP, and to produce a monotonously growing (meta)stable CL. If, on the other hand, the CLs of the SSS are viewed in the opposite way (left portion dropping down and the right one shooting up), then there are no extrema and the point HE is not an HEDCP. In fact, no HEDCP (i.e., no switch in stability) is here desirable since the left branch descending from its maximum M (HEDCP) simply stays unstable, while the right branch is (meta)stable all along. The HEDCP character of HE thus manifests itself only if the SSS is perturbed in the right direction (positive in our example); however, perhaps to "compensate" for this 50% chance, HE is then equivalent to *two* overlapping HEDCPs, a minimum and a maximum. Furthermore, the second-order formula for the slope s at the point HE, eq 27, has to be understood as the derivative of the transverse CL measured "across" the discontinuity, as if this CL were continuous. Obviously, with this interpretation, the nonzero slope is no longer inconsistent with the HEDCP character of the point HE.

The perturbation theory fails badly around T_{HE} where it produces a diverging δw_2; but this is to be expected since the actual "Scott" CL here changes smoothly into a transverse CL for which the perturbation theory was never intended. On the other hand, outside the interval $T_{HE} \pm 6$ K, the agreement with the exact CL is very good.

Perturbation of a SSS with two Scott HEDCPs produces rather complex diagrams (see Figure 15); yet, no new principles are involved, and the pattern of the resulting CL is obvious from eq 31 and 32 even without calculation. In this case the perturbation has been achieved by modifying g_x of the SSS of Figure 13: α_x is reduced by 5%, and β_x increased so as to fix the Scott temperature T_S (eq 24) at 400 K, i.e., *inside* the temperature interval ($T_{HE1}°$, $T_{HE2}°$) of the two Scott HEDCPs. Hence: (i) For $T = 400$ K the perturbed CL should cross the original Scott line. (ii) δw_2 should diverge for $T \to T_{HE}°$. (iii) Since $\delta\beta_x > 0$ and $\delta\Delta\beta = 0$, we should have $\delta g_x > 0$ for $T < T_S$ and $\delta g_x < 0$ for $T > T_S$. (iv) The sign of δw_2 should be identical with that of δg_x for (meta)stable Scott CPs (with $\bar{g} < \bar{g}_{HE}°$, i.e., outside the loop), while it should be opposite for unstable Scott CPs (with $\bar{g} > \bar{g}_{HE}°$, i.e., inside the loop). These qualitative conclusions are confirmed by the computed CL whose relevant portion is enlarged in Figure 15. The displayed line is (meta)stable except for the portion between the two HEDCPs where it is unstable. As before, the perturbation theory gives a very good approximation to the perturbed Scott CL except for the neighborhood of Scott HEDCPs.

A different pattern is generated when the Scott CP (i.e., the switch in polarity of δw_2) is located *outside* the loop. Then the continuous CL of Figure 15 reconfigures and separates into two parts, each on a different side of the Scott composition $w_{2,S}$: one, (meta)stable all along, appears as a deflected Scott CL with a bump on it, whereas the other forms a closed loop divided by two HEDCPs into a (meta)stable outside and an unstable inside portion.

6. Conclusions

Scott critical points (SCPs) represent one of few cases where the critical state equations for a ternary Flory–Huggins system can be solved explicitly and exactly. Their existence requires that the system's interaction parameters satisfy eq 3 and 4, and their composition is then given by eq 1 and 2. They are representative of solutions of two partially miscible polymers.

In principle, the mean polymer–solvent interaction parameter, $\bar{g}$, at an SCP is arbitrary; hence, the locus of SCPs in the 3D space of interaction parameters $\bar{g}$, Δg, and g_x is a half-plane passing through the $\bar{g}$ axis. However, the value of $\bar{g}$ *is* important for other reasons:

(a) If $\bar{g}$ attains the level of $\bar{g}_{HE}$, eq 13, the SCP also becomes a heterogeneous double critical point (HEDCP), which, as usual, marks the boundary between stable and unstable critical points (CPs). Hence, in cases where $\bar{g} > \bar{g}_{HE}$ the SCP is thermodynamically unstable.

(b) If $\bar{g}$ equals $\bar{g}_{HO}$ of eq 17, the triangular phase diagram for the respective temperature contains simultaneously *both* an SCP and a homogeneous double critical point (HODCP) of hyperbolic type 0, i.e., located on the segment 0 of Figure 1. Strictly speaking, the above statement is valid only if $g_x < g_{x,M}$ of eq 20a (usual case). For $g_x > g_{x,M}$ the HODCP should switch to an elliptic type and become also unstable, just as the SCP is here.

(c) If $\bar{g}$ equals $\bar{g}_t$ of eq 16, an unstable SCP coexists with two hyperbolic HODCPs, types 1 and 2. All three CPs share the same polymer volume fraction φ and are located on a linear spinodal parallel to axis 1–2. This implies that the coalescence between the Scott instability and each of the two polymer–solvent instabilities occurs simultaneously at the same temperature and the same φ. With g_x growing, φ diminishes (cf. eq 9b), the linear spinodal of constant φ in the composition diagram shifts upward, and the two HODCPs eventually exit out of the triangle through the two polymer–solvent binary CPs at $g_x = g_{x,Z}$ of eq 15 and at $g_x = g_{x,W}$ of eq 20b, respectively (Figures 6–9).

(d) In a unique case T where the three interaction parameters assume values specified by eq 29 of ref 5, an unstable SCP coexist with *all three* hyperbolic HODCPs, types 0–2, at the same time. Spinodals here reduce to three straight lines, parallel to the triangle sides, drawn at coordinates given by eq 30 of ref 5 (Figure 7 of this paper).

(e) Since the hyperbolic HODCPs generally mark points of coalescence of two two-phase regions into a single one,[5] the above criteria for various HODCPs can be interpreted as criteria for changes in isothermal spinodal (and binodal) patterns of Scott systems. For instance, for the simplest case where only $\bar{g}$ is temperature-dependent, the coalescence occurs first between the two polymer–solvent instabilities if $g_x < g_{x,T}$ (cf. Figure 6a), whereas, in the opposite case, $g_x > g_{x,T}$, both of the polymer–solvent instabilities (if present) first merge, at the same temperature, with the Scott miscibility gap (Figures 8 and 9). More examples can be found in the text.

Hypothetical *strictly Scott systems* (SSS), which satisfy condition 3 and 4 at all temperatures, possess a trivial Scott critical line (SCL)—it is a straight line of constant polymer mixture composition w_2. Of great interest is if and how such a SCL interacts with a "regular" transverse critical line (TCL) well-known, e.g., from quasi-binary ternary systems where the two polymers differ only by their chain lengths ($g_x = \Delta g = 0$). It turns out that the point common to SCL and TCL is always a HEDCP (call it Scott HEDCP). From eq 13 for $\bar{g}_{HE}$, criteria in terms of temperature coefficients for interaction parameters are derived, which predict whether a given system will have two, one, or none such physically significant Scott HEDCP. In the first instance, the interacting TCL usually has a shape of a closed loop (Figure 13), and in the second case it commonly crosses the entire triangle (Figure 12a).

In practice, real systems typically *do not* match eq 3 and 4 at all times; if at all, they may do so perhaps at one temperature (Scott temperature T_S). A first-order perturbation theory of such *Scott systems* is developed, giving shifts in the SCL as a function of systems' deviations from eq 3. Perturbation theory results are simple and agree well with exact computations. The shape of perturbed critical lines and their discontinuity reveal the singular nature of the Scott HEDCP of the above SSSs. Their SCL and TCL in fact *do not intersect* at the HEDCP at all; rather a branch of the SCL abruptly turns into a branch of the TCL, and vice versa. The Scott HEDCP acts merely as a point of contact between two infinitely sharp turns of such critical line portions, which falls apart upon perturbation (cf. Figure 12b). Also, only in this sense a Scott HEDCP behaves as a temperature extremum (as it should); the overall across-the-gap slope of the TCL, on the other hand, is generally nonzero, as apparent from the derived formula as well as from the displayed graphs.

Acknowledgment. Support by the National Science Foundation, Division of Materials Research, Polymers Program, Grant No. DMR-8511494, is gratefully acknowledged. We also thank M. Rozniak for his technical help.

Appendix

Proving that the point HE, eq 13, is a *heterogeneous double critical point* (HEDCP) is not trivial since some expressions in the HEDCP criterion become of 0/0 type and have to be carefully evaluated.

The easiest way is to employ the criterion in Korteweg's form, eq 9 of ref 7. It is apparent that both ratios $\langle r^2\xi^3\rangle^3/\langle r\xi\rangle$ and $\langle r^2\xi^3\rangle/\langle r\xi\rangle$ appearing in this equation have to go to zero as the composition approaches $w_{2,S}$ since the ratio $\langle r^2\xi^3\rangle/\langle r\xi\rangle^3$ is known to be in this limit finite (cf. eq 5). After the rest of the terms from eq 1, 8, 9, and 13 are substituted, the criterion turns out to be satisfied.

In the more general version of the HEDCP criterion, eq 17 of ref 7, it is the derivative (cf. eq 21 of ref 7)

$$\frac{d\xi}{d\eta} = \frac{\varphi_2 r_2^2 \xi^2 P - \varphi_1 r_1^2 \xi^{-2} M}{4(1 - \varphi_2 r_2 P)} \tag{A1}$$

that becomes 0/0 at the point HE. It can be evaluated by applying the L'Hospital rule, i.e., by differentiating both the numerator and the denominator and employing the known relations among the differentials, eq 10–12. With the resulting limit

$$(d\xi/d\eta)_{HE} = \rho_1(\rho_1 + \rho_2)/12 \tag{A2}$$

this alternate form of the HEDCP criterion becomes satisfied as well.

The criterion for the *triple critical point* (cf. eq 22 of ref 7) also contains another term of 0/0 type, namely the second derivative $d^2\xi/d\eta^2$. Using an analogous approach as above for $d\xi/d\eta$, the first differential of the numerator at the point HE is found to be nonzero while that of the

denominator approaches zero. Since all the other terms of the criterion remain finite, the diverging second derivative $d^2\xi/d\eta^2$ indicates that the Scott HEDCP cannot ever be a triple CP.

References and Notes

(1) Scott, R. L. *J. Chem. Phys.* **1949**, *17*, 279.
(2) Flory, P. J. *Principles of Polymer Chemistry*; Cornell University Press: Ithaca, NY, 1953; Chapters XII and XIII.
(3) Karam, H. J. Compatibility of Two Polymers With and Without Solvent. In *Polymer Compatibility and Incompatibility*; Šolc, K., Ed.; Harwood Academic Publishers: New York, 1982; pp 93-106.
(4) Šolc, K. *Macromolecules* **1986**, *19*, 1166.
(5) Šolc, K.; Yang, Y. C. *Macromolecules* **1988**, *21*, 829.
(6) Šolc, K.; Yang, Y. C. To be published.
(7) Šolc, K. *Macromolecules* **1987**, *20*, 2506.
(8) Tompa, H. *Trans. Faraday Soc.* **1949**, *45*, 1142.
(9) Korteweg, D. J. *Sitzungsber. Kais. Akad. Wiss. Wien, Math.-Naturwiss. Kl., 2 Abt. A* **1889**, *98*, 1154.
(10) Zeman, L.; Patterson, D. *Macromolecules* **1972**, *5*, 513.
(11) The extremal terms used here refer to figures as they are drawn. Their interpretation in terms of physical quantities can go either way: For instance, for the case of $\bar{\beta} > 0$, they also relate directly to the temperature; however, they have to be switched (a maximum for a minimum and vice versa) when discussed in terms of $\bar{g}$.
(12) Note that the system's trajectory, although linear in the actual interaction space, transforms in the compressed coordinates of Figure 4 into a hyperbolic curve diverging for $\varphi \to 0$ (i.e., $T \to 0$).

Polymer–Polymer Interaction Parameter in the Presence of a Solvent[1]

Margarita G. Prolongo

Departamento de Materiales y Producción Aerospacial, E.T.S. Ingenieros Aeronáuticos, Universidad Politécnica de Madrid, 28040 Madrid, Spain

Rosa M. Masegosa

Departamento de Química, E.U.I.T. Aeronáutica, Universidad Politécnica de Madrid, 28040 Madrid, Spain

Arturo Horta*

Departamento de Química Física, Facultad de Ciencias, Universidad a Distancia (UNED), 28040 Madrid, Spain.

Received January 16, 1989; Revised Manuscript Received April 3, 1989

ABSTRACT: A method is proposed to calculate the polymer–polymer interaction parameter (χ) from measurements performed on ternary systems composed of the polymer pair plus a solvent or probe. The usual methods of extracting χ from such measurements do not provide a true polymer–polymer interaction parameter because of the approximation of writing the residual chemical potential of the solvent in the ternary system as a sum of binaries. The equation-of-state theory gives a truly ternary chemical potential and can thus avoid such an approximation. The expressions needed to calculate the true polymer–polymer χ from such ternary theory are given. They are applied to obtain χ of the system PS + PVME from literature data determined by vapor sorption (VP) and inverse gas chromatography (IGC), with different solvents and probes. The results show that the method here proposed (a) gives χ from VP independent of the solvent used; (b) explains why the χ determined by IGC is probe dependent and predicts a correlation which allows for a probe-independent value of χ to be extracted, (c) shows that this probe-independent χ value from IGC is practically the same obtained from VP (by extrapolation to vanishing solvent concentration).

Introduction

In the last years, an important part of the applied polymer research has been aimed at preparing polymer blends to get new materials having improved properties and/or lower cost. The increasing interest in this field has led to the discovery of an ever-expanding number of compatible polymers. Miscibility in a polymer blend is controlled, as in any other mixture, by thermodynamic factors. Due to the extremely low values of the combinatorial entropy, a great many polymer pairs are incompatible, since a slightly positive mixing enthalpy is enough to prevent miscibility. Because of this, the majority of compatible polymer pairs are due to specific interactions such as hydrogen bonds.[2,3]

In the classical theory of Flory and Huggins,[4] the polymer–polymer interaction parameter χ_{ij} is used to describe the interaction between the two components of the blend. In general, the convention followed with regard to the values of this parameter is that high values are indicative of unfavorable interactions between the two components of the polymer blend, low values are indicative of slightly favorable interactions, and negative values appear when there are strong specific interactions between the two polymers.[3]

The polymer–polymer interaction parameter χ_{ij} can be determined by several techniques.[2,5,6] Among the most oftenly used ones are: inverse gas chromatography (IGC), vapor sorption (VP), osmometry, viscometry, and light scattering, melting point depression, small-angle X-ray scattering, and small-angle neutron scattering.

The techniques aforementioned can be divided in two groups, depending on the way χ_{ij} is obtained:

(1) Techniques that obtain χ_{ij} from measurements performed on the binary polymer–polymer system. Such are the melting point depression, whose usefulness is limited to the case in which one of the polymers in the mixture is crystalline and it gives χ_{ij} at a single temperature, the small-angle X-ray scattering and small-angle neutron scattering, whose usefulness is limited by the availability of the equipment and requires the deuteration of samples.

(2) Techniques more oftenly used, in which χ_{ij} is obtained from measurements performed on a ternary poly-

0024-9297/89/2222-4346$01.50/0